doi:10.1246/cl.2011.1095
Published on the web September 23, 2011

One-pot Simultaneous Synthesis of Au–Pt Core–Shell Nanoparticles Protected by a Nafion® Ionomer in an Aqueous Solution

Naoki Toshima,* Hideo Naohara, Takahiro Yoshimoto, and Yasuaki Okamoto
Department of Applied Chemistry, Tokyo University of Science Yamaguchi, Sanyo-Onoda, Yamaguchi 756-0884

(Received June 23, 2011; CL-110525; E-mail: toshima@ed.yama.tus.ac.jp)

We successfully synthesized Au–Pt bimetallic core–shell nanoparticles by simultaneous reduction covered with a perfluorinated sulfonic acid ionomer (PFSA) in an aqueous solution. The core–shell structure was confirmed by energy-dispersive X-ray spectrometry line analysis. Electrocatalytic activity of the Au–Pt nanoparticles for oxygen reduction reaction was higher than those of PFSA-covered Pt nanoparticles and a conventional carbon-supported Pt catalyst.

Structure controlled bi-/multimetallic nanoparticles have attracted much attention due to their specific chemical and physical properties and have been used widely in various applications such as catalysis, biochemistry, magnetism, and photonics.[1–7] Controlling the structure and composition of bi-/multimetallic nanoparticles has been established by chemical preparation methods such as simultaneous and successive reduction with protecting agents in the solution[8–13] and electrochemical methods such as galvanic displacement of underpotentially deposited (UPD) Cu adatoms on a substrate metal surface by another metal monolayer.[14–17] Precious metals, especially Pt, are known to be good catalysts for various reactions, and it has been reported that ultrathin layers deposited on a foreign core (substrate) metal show better catalytic activity than that of simple alloys.[18–20] Au–Pt nanoparticles have been synthesized by simultaneous and successive reduction with various protecting agents. They showed better electrocatalytic activity for oxidation of small organic molecules and reduction of oxygen than that of a conventional carbon-supported Pt (Pt/C) catalyst.[21–24] Protecting agents, however, sometimes deactivate the catalytic/electrocatalytic reactions or inhibit the diffusion of reactants and products on the nanoparticle surface due to their strong interaction with the surface. Recently, we have successfully prepared Pt nanoparticles and Pd–Pt bimetallic core–shell nanoparticles in an aqueous solution with a nanonetwork structure using a perfluorinated sulfonic acid ionomer (PFSA) directly as the protecting agent and showed their good electrocatalytic activity for oxygen reduction reaction (ORR).[25,26] PFSA, for example Nafion®, which has good proton conductivity, gas permeability, and chemical stability, is used not only for the electrolyte membrane but also for the catalyst layer as an ionomer in fuel cell. Therefore, when PFSA is used directly as the protecting agent, additional procedures to remove it from the nanoparticle surface are not required for practical applications.

In this study, we successfully tried to synthesize PFSA-covered Au–Pt core–shell (Au/Pt/PFSA) nanoparticles by simultaneous reduction in an aqueous solution. The structure, local composition, and electrocatalytic activity for ORR of the Au/Pt/PFSA nanoparticles were investigated by transmission electron microscopy (TEM), scanning transmission electron microscopy (STEM), energy-dispersive X-ray spectrometry (EDS), and voltammetry.

The Au/Pt/PFSA nanoparticles were synthesized from hydrogen tetrachloroaurate(III) and hydrogen hexachloroplatinate(IV) hexahydrate (Wako Pure Chemical Industries) and Nafion® DE1020CS PFSA dispersion (DuPont Fuel Cells) by simultaneous reduction. After a fixed volume of the PFSA solution ($R = 0.5\%$) was mixed with deoxidized Milli-Q water for 30 min, the solutions of hydrogen tetrachloroaurate(III) and hydrogen hexachloroplatinate(IV) hexahydrate were added to the mixture, followed by stirring the solution for 1 h under an atmosphere of nitrogen in the dark. R denotes a molar ratio of monomer unit of PFSA to metals. Sodium tetrahydroborate was added to the mixed solution at 0 °C, and then the mixed solution was kept stirring for 1 h at 0 °C. The Au/Pt/PFSA nanoparticles were purified by filtration with ultrafilter (Advantec, Q0100076E) by washing with Milli-Q water several times until no chloride ions were detected in the filtered solution. Finally, the dispersion was concentrated to 0.05–0.1 wt % of metal content for the electrochemical measurements.

The electrochemical measurements were carried out using a rotating disk electrode (RDE) in an Ar- or O_2-saturated 0.1 mol L^{-1} perchloric acid solution. A conventional three-electrode cell was equipped with a reversible hydrogen electrode (RHE) and platinized foil as the reference and counter electrodes, respectively. The sample electrode was prepared by direct dropwise addition of 3.92 μg platinum in the Au/Pt/PFSA nanoparticle solutions onto a rotating electrode surface (0.196 cm^2) made of glassy carbon and then dried under a nitrogen flow. The actual Pt content in the colloidal solution was analyzed by inductively coupled plasma atomic emission spectrometry (ICP-AES). TEM and STEM/EDS measurements were carried out using a JEM2010F and JEM2100F, respectively.

UV–visible absorption spectroscopy is a useful method to confirm both the degree of consumption of precursors by monitoring their ligand-to-metal or metal-to-ligand charge-transfer transitions and the formation of a band structure of nanoparticles by monitoring the plasmon band or the broad tailing absorption in the range from UV to visible region resulting from the inter- and intraband charge-transfer transitions. Figure 1 shows UV–visible spectra of the solutions of metal precursor ions, Au nanoparticles and the Au/Pt/PFSA nanoparticles (Au/Pt denotes the molar ratio of Au to Pt). A strong absorption peak and a weak shoulder assigned to ligand-to-metal charge-transfer transitions of $[PtCl_6]^{2-}$ were observed at 270 and 370 nm, respectively, before the reduction.[27] In the case of Au nanoparticles, a strong absorption peak assigned to the plasmon absorption of Au was observed at 520 nm. On the other hand, only broad tailing absorptions were observed in the case of Au/Pt/PFSA nanoparticles prepared by the simultaneous reduction method even at every Au/Pt ratios. No absorption peak due to the Au plasmon absorption at 520 nm was observed. This suggests that Au particles were covered by Pt atoms even when prepared by simultaneous reduction in the PFSA aqueous solution. These

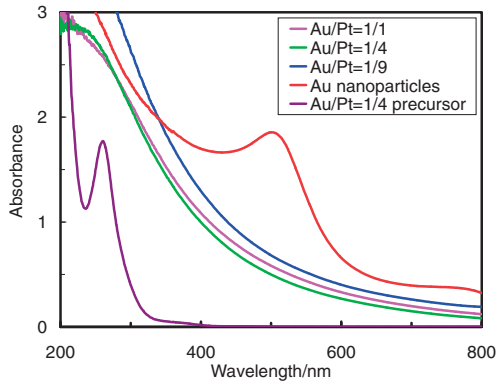

Figure 1. UV–visible spectra of the solution of Au and Pt precurcor ions, Au nanoparticles, and the Au/Pt/PFSA nanoparticles (Au/Pt = 1/1, 1/4, and 1/9).

results are in good agreement with the previous reports that the Au–Pt core–shell structure was formed by simultaneous reduction in the poly(*N*-vinyl-2-pyrrolidone) (PVP) solution.[11] This suggests that PFSA works well as the protecting agent for forming metal nanoparticles in the same way as in the cases of the Pt/PFSA and the Pd/Pt/PFSA nanoparticles.[25,26]

The structures and local composition of the Au/Pt/PFSA nanoparticles were characterized by TEM and STEM. Figure 2 shows TEM images of the Au/Pt/PFSA (Au/Pt = 1/4) nanoparticles after the purification. Uniform nanoparticles formed nanowires and the nanowires construct a nanonetwork after the purification of colloids in the same way as in the cases of the Pt/PFSA and the Pd/Pt/PFSA nanoparticles.[25,26] The mean diameter of nanoparticles was 5.3 ± 0.9 nm. Each nanoparticle showed different lattice direction, and the neighboring nanoparticles were not connected at the specific faces of each other. Therefore, the growth of the nanowires did not depend on the direction of the crystal lattice. The nanonetwork of the Au/Pt/PFSA nanoparticles was also confirmed by SEM to retain a self-organized three-dimensional network structure even in a dried film. Porous structure of the catalyst layer should enhance the efficiency of active sites and the diffusion of reactants/products.

The intensity of the HAADF image reflects Z^2 (Z: atomic number) and the concentration of the elements,[28] so that a distribution of elements can be observed as an actual image. Figure 3 shows the HAADF image of the Au/Pt/PFSA (Au/Pt = 1/4) nanoparticles. The less bright area was observed on the rim of the nanoparticles, but it is difficult to distinguish Pt ($Z = 78$) from Au ($Z = 79$) due to adjoining Z. Local EDS analysis along the line in the HAADF image, as inset curves in the image, clearly shows the localization of Pt and F on the surface of the nanoparticles. The line profiles of EDS suggest the formation of Au–Pt core–shell structure. A small amount of Au was detected on the surface, indicating that Pt might not perfectly cover Au. The Pt nanoparticles independently depositing on the Au nanoparticles were not observed by EDS mapping over a wide area. The atomic ratios of Au/Pt confirmed by ICP and EDS analyses over a wide area were 1/3.9 and 1/4, respectively. The coincidence of the values suggests that all precursors are reduced to nanoparticles. The STEM measurements indicate that the PFSA-protected nanowires and nanonetwork structure with the Au–Pt core–shell structure were synthesized by simultaneous reduction of the precursor ions in the presence of PFSA in an aqueous solution at room temperature. More detail information about the Au–Pt core–shell structure is under investigation by X-ray and high-resolution STEM measurements.

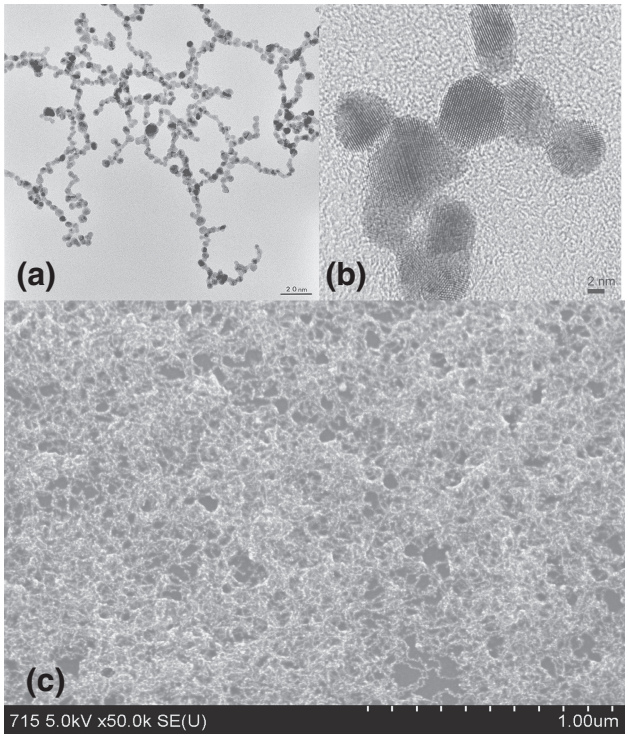

Figure 2. Formation of nanowires and nanonetwork structure after purification: (a) TEM images of the Au/Pt/PFSA (Au/Pt = 1/4) nanoparticles, (b) magnified image of (a), and (c) SEM image of the Au/Pt/PFSA (Au/Pt = 1/4) nanoparticles.

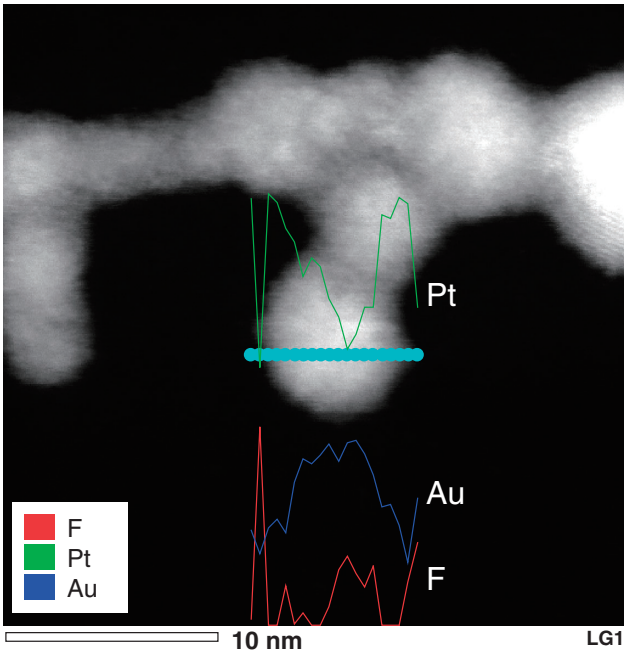

Figure 3. A HAADF image of the Au/Pt/PFSA (Au/Pt = 1/4) nanoparticles. Insets are the EDS analysis along a line in the figure.

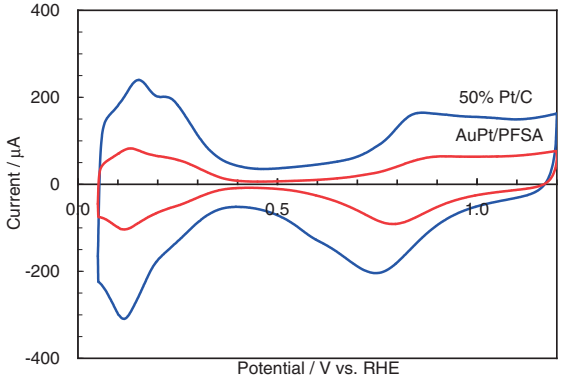

Figure 4. Cyclic voltammograms of the Au/Pt/PFSA (Au/Pt = 1/4) and the Pt/C catalyst in 0.1 mol L^{-1} perchloric acid solution.

The equilibrium potential of Au is much more positive than that of Pt,[29] so that the reduction and the nuclei formation of Au should be faster than those of Pt, which induce formation of core–shell nanoparticles. And also, it is known that surface adsorbates induce the core–shell structure.[17] It was reported that in Nafion® adsorbed on a Pt surface, the behavior of sulfonate anions was similar to that of sulfate and/or hydrogensulfate anions,[30] and sulfate anions prefer the Pt surface to the Au surface.[31] If an affinity of sulfonate anions to Pt is stronger than to Au, PFSA might induce formation of the Au–Pt core–shell structure.

Figure 4 shows cyclic voltammograms (CVs) of the Pt/C catalyst and the Au/Pt/PFSA nanoparticles observed in an Ar-saturated 0.1 mol L^{-1} perchlolic acid solution. The electrochemical surface area (ECSA) of the Au/Pt/PFSA (Au/Pt = 1/4) nanoparticles, calculated by the hydrogen adsorption, was 38.0 m^2 g-Pt^{-1}. This value is lower than that of the Pt/C (68.3 m^2 g-Pt^{-1}) due to large particle size but slightly higher than that of the Pt/PFSA (32.1 m^2 g-Pt^{-1}).[25] The core–shell structure enhances the efficiency of Pt. The cathodic peak due to Pt oxide reduction of the Au/Pt/PFSA (Au/Pt = 1/4) nanoparticles was 0.789 V, which was shifted to positive direction by 0.046 V than that of the Pt/C catalyst. This suggests that the stability for oxide formation and the electrocatalytic activity for oxygen reduction of the Au/Pt/PFSA (Au/Pt = 1/4) nanoparticles should be improved compared to the Pt/PFSA nanoparticles and the Pt/C catalyst. The CV of the Au/Pt/PFSA (Au/Pt = 1/1) nanoparticles up to 1.6 V showed a cathodic peak due to the reduction of Au oxide, while no reduction peak was observed at the Au/Pt/PFSA (Au/Pt = 1/4) and Au/Pt/PFSA (Au/Pt = 1/9) nanoparticles. This indicated that Au atoms exposed on the surface of the Au/Pt/PFSA (Au/Pt = 1/1) nanoparticles.

Electrocatalytic activity for oxygen reduction of the Au/Pt/PFSA (Au/Pt = 1/4) nanoparticles was investigated with a rotating disk electrode in an 0.1 mol L^{-1} O_2-saturated perchloric acid solution. The kinetic current (I_k) of the Au/Pt/PFSA (Au/Pt = 1/4) nanoparticles analyzed by the Koutecky–Levich plot was 1.04 mA at 0.9 V. The calculated mass activity (MA) and specific surface activity (SSA) were 0.27 A mg-Pt^{-1} and 0.7 mA cm^{-2}, respectively, which were larger than those of the Pt/PFSA nanoparticles and the conventional Pt/C catalyst. The geometric effect of the core–shell structure and the alloying effect enhance ORR activity.

In conclusion, we successfully synthesized Au–Pt core–shell nanoparticles with the nanonetwork structure, covered with PFSA, by simultaneous reduction in the aqueous solution at room temperature. The core–shell structure was confirmed by EDS line analysis. The difference between Au and Pt in the equilibrium potential should induce the formation of the core–shell structure. The electrocatalytic activity of Au–Pt nanoparticles for ORR was higher than those of the Pt/PFSA nanoparticles and the conventional Pt/C catalyst.

References

1 N. Toshima, T. Yonezawa, *New J. Chem.* **1998**, *22*, 1179.
2 N. Toshima, Y. Shiraishi, T. Teranishi, M. Miyake, T. Tominaga, H. Watanabe, W. Brijoux, H. Bönnemann, G. Schmid, *Appl. Organomet. Chem.* **2001**, *15*, 178.
3 T. Teranishi, N. Toshima, in *Catalysis and Electrocatalysis at Nanoparticles Surfaces*, ed. by A. Wieckowski, E. R. Savinova, C. G. Vayenas, Marcel Dekker, Inc., New York, **2003**, Chap. 11.
4 *Metal Nanoclusters in Catalysis and Materials Science: The Issue of Size Control*, ed. by B. Corain, G. Schmid, N. Toshima, Elsevier, Amsterdam, **2008**.
5 R. Ferrando, J. Jellinek, R. L. Johnston, *Chem. Rev.* **2008**, *108*, 845.
6 C. Burda, X. Chen, R. Narayanan, M. A. El-Sayed, *Chem. Rev.* **2005**, *105*, 1025.
7 V. I. Pârvulescu, C. Hardacre, *Chem. Rev.* **2007**, *107*, 2615.
8 N. Toshima, M. Harada, T. Yonezawa, K. Kushihashi, K. Asakura, *J. Phys. Chem.* **1991**, *95*, 7448.
9 N. Toshima, T. Yonezawa, K. Kushihashi, *J. Chem. Soc., Faraday Trans.* **1993**, *89*, 2537.
10 N. Toshima, M. Harada, Y. Yamazaki, K. Asakura, *J. Phys. Chem.* **1992**, *96*, 9927.
11 T. Yonezawa, N. Toshima, *J. Mol. Catal.* **1993**, *83*, 167.
12 M. Harada, K. Asakura, N. Toshima, *J. Phys. Chem.* **1993**, *97*, 5103.
13 Y. Wang, N. Toshima, *J. Phys. Chem. B* **1997**, *101*, 5301.
14 J. Zhang, Y. Mo, M. B. Vukmirovic, R. Klie, K. Sasaki, R. R. Adzic, *J. Phys. Chem. B* **2004**, *108*, 10955.
15 K. Sasaki, J. X. Wang, H. Naohara, N. Marinkovic, K. More, H. Inada, R. R. Adzic, *Electrochim. Acta* **2010**, *55*, 2645.
16 K. Sasaki, H. Naohara, Y. Cai, Y. M. Choi, P. Liu, M. B. Vukmirovic, J. X. Wang, R. R. Adzic, *Angew. Chem., Int. Ed.* **2010**, *49*, 8602.
17 H. Yang, *Angew. Chem., Int. Ed.* **2011**, *50*, 2674.
18 G. A. Somorjai, Y. Li, *Introduction to Surface Chemistry and Catalysis*, John Wiley & Sons, **1994**.
19 K. Uosaki, S. Ye, H. Naohara, Y. Oda, T. Haba, T. Kondo, *J. Phys. Chem. B* **1997**, *101*, 7566.
20 T. Kondo, M. Shibata, N. Hayashi, H. Fukumitsu, T. Masuda, S. Takakusagi, K. Uosaki, *Electrochim. Acta* **2010**, *55*, 8302.
21 B. N. Wanjala, J. Luo, R. Loukrakpam, B. Fang, D. Mott, P. N. Njoki, M. Engelhard, H. R. Naslund, J. K. Wu, L. Wang, O. Malis, C.-J. Zhong, *Chem. Mater.* **2010**, *22*, 4282.
22 Z. Xu, C. E. Carlton, L. F. Allard, S.-H. Yang, K. Hamad-Schifferli, *J. Phys. Chem. Lett.* **2010**, *1*, 2514.
23 S. Guo, J. Li, S. Dong, E. Wang, *J. Phys. Chem. C* **2010**, *114*, 15337.
24 M. Shao, A. Peles, K. Shoemaker, M. Gummalla, P. N. Njoki, J. Luo, C.-J. Zhong, *J. Phys. Chem. Lett.* **2011**, *2*, 67.
25 H. Naohara, T. Yoshimoto, N. Toshima, *J. Power Sources* **2010**, *195*, 1051.
26 H. Naohara, Y. Okamoto, N. Toshima, *J. Power Sources* **2011**, *196*, 7510.
27 A. Henglein, B. G. Ershov, M. Malow, *J. Phys. Chem.* **1995**, *99*, 14129.
28 P. D. Nellist, S. J. Pennycook, *Ultramicroscopy* **1999**, *78*, 111.
29 *Standard Potentials in Aqueous Solution*, ed. by A. J. Bard, R. Parsons, J. Jordan, Marcel Dekker, Inc., New York, **1985**.
30 R. Subbaraman, D. Strmcnik, V. Stamenkovic, N. M. Markovic, *J. Phys. Chem. C* **2010**, *114*, 8414.
31 *Nanoscale Probes of the Solid/Liquid Interface*, ed. by A. A. Gewirth, H. Siegenthaler, Kluwer, Dordrecht, **1995**.

